Polymer, 1991, Vol. 32, 109–120

Influence of molecular structure and composition of ethylene–vinyl acetate copolymers on morphology and tensile elastic behaviour of injection-moulded samples of polyamide-6 based blends

M. L. Addonizio, L. D'Orazio and E. Martuscelli*
Istituto di Ricerche su Tecnologia dei Polimeri e Reologia del CNR, via Toiano, 6 80072 Arco Felice (Napoli), Italy
(Received 6 October 1989; accepted 18 December 1989)

A study of the mode and state of dispersion of ethylene–vinyl acetate (EVA) copolymers, differing in molecular mass and, for a given molecular mass, in vinyl–acetate content (wt/wt), in injection-moulded samples of polyamide-6 based blends is reported. An attempt has been made to correlate molecular structure and composition of EVA copolymers to shape and size of domains of dispersed phase and elastic and tensile yielding behaviour of blended materials.

(Keywords: polyamide-6; ethylene–vinyl acetate copolymers; blends; morphology; properties)

INTRODUCTION

The results of an investigation concerning the study of the influence of composition, post-blending processing (extrusion and injection moulding) and processing conditions (temperature and residence time) on the rheological behaviour, overall morphology and impact properties of blends of nylon-6 (polyamide-6, PA6) and ethylene-*co*-vinyl acetate (EVA) copolymers were reported in previous papers[1,2]. From such studies aimed at correlating processing, morphology and properties in the PA6/EVA system, we concluded that for this incompatible polymer blend the mechanical response is determined by a combination of interrelated factors such as phase viscosity ratio, molecular mass, molecular mass distribution and molecular structure of EVA copolymers, as well as blend composition.

In order to optimize some of the factors identified above, keeping the others almost constant, we blended PA6 with several EVA copolymers differing in molecular mass and, for a given molecular mass, in the vinyl acetate content (from 20% wt/wt up to 40% wt/wt). The results of a study dealing with the rheological behaviour in the molten state of this type of blend and with the mode and state of dispersion of the minor component developed in extruded blend samples as functions of both molecular mass and composition of the EVA copolymers have already been reported[3].

The application of the Cross–Bueche equation[4] revealed that the values of the zero shear viscosity η_0 of PA6/EVA blends were mainly dependent on the molecular mass of EVA copolymers. Over the whole range of temperatures explored (230, 240, 250 and 260°C), the η_0 values of blends containing copolymer with low molecular mass were found to be lower than that of plain PA6, whereas η_0 values higher than that of plain PA6 were shown by the blends containing EVA copolymer having comparatively intermediate and high molecular mass. The values of characteristic relaxation time α for PA6 were always lower than those of PA6/EVA blends, indicating that for the blends the transition from Newtonian to pseudoplastic flow starts at values of the shear rate $\dot{\gamma}$ lower than that of plain PA6. Moreover it was observed that, at a given temperature, for blend samples, η_0 and α increase with increasing (i) molecular mass of the copolymer for a given percentage of vinyl acetate and (ii) percentage of vinyl acetate of the copolymer for a given molecular mass. The activation energy for viscous flow ΔE^* calculated for PA6/EVA blends was found to be higher than that of plain PA6, indicating growth of the volume of the flow element and supporting the flow model of melts of incompatible blends proposed by Utraki and Kamal[5].

The order of dispersion coarseness of the minor component in the resulting extruded filaments was mainly determined by EVA melt viscosity. For a given content of vinyl acetate along the EVA chain a finer dispersion was developed in blends containing copolymers with comparatively higher molecular mass. For a given EVA molecular mass, an increase of vinyl acetate content along the copolymer chain from 20% (wt/wt) to 30% (wt/wt) promoted finer EVA dispersion only in the case of copolymer having a higher melt viscosity. An anisotropic distribution of dispersed phase was moreover observed. The EVA particle size was found to increase on going from the skin towards the core of the filaments with a characteristic gradient. On the other hand, in the outer region of the filaments the EVA minor component segregated in ellipsoidal and/or cylindrical shaped domains, the deformation undergone by EVA droplets depending on the particle radius.

Pursuing the goal of optimizing the molecular mass and the vinyl acetate content of the EVA copolymers in

* To whom correspondence should be addressed

0032-3861/91/010109–12

PA6 based blends, in the present paper we present the results of a systematic study carried out to determine the influence of molecular structure and composition of the EVA minor component on the morphology and elastic and tensile yielding behaviour in injection-moulded samples. The final target of the research has always been that of tailoring the phase morphology of PA6/EVA blends and the ultimate properties of the processed blended material.

EXPERIMENTAL

Materials

The materials used in this study were the following: nylon-6 (PA6) produced by SNIA with a number-average molecular weight $\bar{M}_n = 18\,000$ and seven different commercial ethylene–vinyl acetate (EVA) copolymers kindly supplied by SNIA.

The codes of the copolymers, the weight percentage of vinyl acetate, the melt flow index, the observed melting temperature (T_m) and the glass transition temperature (T_g) are listed in *Table 1* together with the T_m and T_g values of PA6.

Blending and sample preparation

The blends, all containing 10 wt% EVA, were obtained by extruding the two components in a double-screw extruder (Creusot–Loire, 56 mm diameter) operating at 83 rpm and at a temperature of 240°C.

The extrudate materials were injection moulded by means of an injection press (Biraghi) at a temperature of 230°C with a processing cycle of 30 s, in sheets of 1 mm thickness. The temperature of the mould was 40°C. From the sheets obtained, dumbbell-shaped specimens (DIN 53448 T2) for morphological and tensile tests were cut by means of a punch press. Before examining, all the specimens were conditioned in water at 90°C in order to obtain the same amount of absorbed water (about 3 wt%) according to a procedure described elsewhere[6].

Techniques

Calorimetric measurements. The glass transition temperatures (T_g), the observed melting temperatures (T'_m) and the crystallinity index of pure PA6 and its blends with EVA copolymers were obtained by using a Mettler TA 3000 differential scanning calorimeter.

The following procedure was used. The samples of pure PA6 and PA6/EVA blends (about 15 mg) were heated from −100°C up to 300°C at a rate of 20°C min^{-1} and the heat (dH/dt) evolved during the scanning process was recorded as a function of temperature. The T_g was taken as the temperature corresponding to 50% of the transition. The observed melting temperature T'_m and the apparent enthalpies of fusion ΔH^* were obtained from the inflection point and area of the melting peaks respectively.

The crystallinity index of PA6 phase (X_c(PA6)) and of overall blend (X_c(blend)) was calculated by means of the following relations:

$$X_c(\text{PA6}) = \frac{\Delta H^*(\text{PA6})}{\Delta H^\circ(\text{PA6})} \qquad X_c(\text{blend}) = \frac{\Delta H^*(\text{blend})}{\Delta H^\circ(\text{PA6})}$$

where ΔH^*(PA6) is the apparent enthalpy of fusion per gram of PA6 in the blend; ΔH°(PA6) is the heat of fusion per gram of 100% crystalline PA6 (from literature data[7] $\Delta H^\circ(\text{PA6}) = 188\ \text{J g}^{-1}$) and ΔH^*(blend) is the apparent enthalpy of fusion per gram of blend.

Wide-angle X-ray scattering. WAXS patterns (Cu Kα, Ni-filtered radiation) were collected by a Rigaku Denki MicroLaue camera (sample–film distance 4 cm) and analysed by Officina Elettrotecnica di Tenno microcomputerized densitometer (model AA 750) (scanning plane xy, resolving power up to 1/200 mm).

From densitometer traces the γ form index, I_γ, was calculated for plain PA6 and PA6 crystallized in the presence of EVA copolymers. The following Kyotami[8] equation was used:

$$I_\gamma = \frac{H_2}{H_1 + H_2 + H_3}$$

where H_1 and H_3 are the heights of the (2 0 0) and (0 0 2), (2 0 2) crystalline reflections of α form and H_2 is the height of the (0 0 1) crystalline reflection of PA6 γ form, in 2θ region between 20 and 25°.

Mode and state of dispersion of the minor component. The mode and state of dispersion of the minor component were investigated by means of a scanning electron microscope (Philips SEM 501). The morphological analysis was performed on surfaces microtomed perpendicularly and tangentially to the mould flow direction and on cryogenic fracture surfaces of the dumbbell-shaped specimens after coating with gold–palladium. To better elucidate the mode and state of dispersion of the EVA copolymers into the PA6 matrix, selective dissolution of the dispersed phase was also carried out according to a method described in a previous paper[1].

Mechanical tensile behaviour. By utilization of an Instron machine (model 1122), at a constant cross-head speed of 20 mm min^{-1} and room temperature, the stress–strain curves for pure PA6 and PA6 crystallized in the presence of EVA copolymers were obtained.

From such curves, the Young's modulus E, the stress at yield σ_y and the elongation at yield ε_y were calculated on an average of 10 specimens.

Table 1 Molecular characteristics, glass transition temperature (T_g) and observed melting temperatures (T'_m) of plain polyamide-6 (PA6) and ethylene–vinyl acetate (EVA) copolymers

Code	Vinyl acetate (% wt/wt)	Melt index (g/10 min)	T_g (°C)	T'_m (°C)
PA6	–	–	42	222
EVA1	20	300–500	−19	80
EVA2	20	3–4	−15	88
EVA3	30	300–500	−19	60
EVA4	30	30–40	−17	60
EVA5	30	3–4	−15	63
EVA6	35	30–40	−16	53
EVA7	40	30–40	−15	55

RESULTS AND DISCUSSION

Thermal behaviour and crystallinity

From the d.s.c. thermograms of PA6/EVA injection-moulded blends, two distinct glass transition temperatures (T_g) are clearly shown; these T_g are located in the ranges −11 to −9°C and 42 to 45°C and are to be attributed to EVA copolymer and PA6 phase respectively.

Table 2 Glass transition temperature (T_g) and observed melting temperatures (T'_m) of plain polyamide-6 (PA6) and the PA6/ethylene–vinyl acetate (EVA) copolymer blends

Code	T_g^* (°C)	T_g (°C)	T'^*_m (°C)	T'_m (°C)
PA6	–	42	–	222
PA6/EVA1	−9	44	80	225
PA6/EVA2	−9	45	90	222
PA6/EVA3	−9	45	85	224
PA6/EVA4	−10	42	75	223
PA6/EVA5	−9	45	80	222
PA6/EVA6	−11	44	70	222
PA6/EVA7	−9	44	85	222

T_g, T'_m = glass transition temperature and observed melting temperature of PA6 in the blends
T_g^*, T'^*_m = glass transition temperature and observed melting temperature of EVA in the blends

By comparing the T_g values shown by the neat polymers with the T_g values shown by the components in the blends, it can be seen that the EVA T_g results shifted about 10°C to higher temperatures (see *Tables 1* and *2*), suggesting that dissolution of the low-molecular-mass EVA into the PA6 matrix could have occurred. The calorimetric measurements performed reveal, moreover, that both plain PA6 and PA6 crystallized in the presence of EVA copolymer show multiple fusion peaks probably due to recrystallization phenomena in the course of heating and polymorphic transition. In *Table 2* the PA6 melting temperature (T'_m) corresponding to the highest temperature peaks are reported. It seems reasonable to suppose that such temperatures are characteristic of the melting of the more stable α crystalline form of PA6. As shown in *Table 2*, the T'_m value of the PA6 crystallized in the presence of EVA copolymers closely approaches that of plain PA6. This finding, according to the results reported in previous papers[2,3], confirms that the PA6 phase in the case of PA6/EVA blend does not dissolve any appreciable amount of EVA molecules. Endothermic peaks due to the melting of ethylene blocks of EVA copolymers in PA6/EVA blend thermograms are also observable; the corresponding temperatures are reported in *Table 2*. By comparing the T'_m values exhibited by the neat EVA copolymers (T'_m) with the T'_m values exhibited by the EVA copolymers in the blends (T'^*_m) it can be seen that the T'^*_m values depend strongly on the VAc content along the EVA chain and, for a given VAc content (30% wt/wt), on the copolymer molecular mass (see *Tables 1* and *2*).

As a matter of fact, in the case of the blends containing EVA copolymers having 20% wt/wt of VAc along their chains (EVA1 and EVA2), irrespective of their molecular mass, the T'^*_m values closely approach the T'_m values. With increasing VAc content along the EVA chain, the T'^*_m values overcame the T'_m values. It should be pointed out that, in the case of the blends containing EVA copolymers with 30% wt/wt of VAc along their chain, the T'^*_m increase depends on the EVA molecular mass. As a matter of fact the T'^*_m value increases with decreasing copolymer molecular mass. The highest increase of the observed melting temperature of the EVA component in the blends is shown by the EVA copolymer having the largest VAc content along its chain (EVA7) (see *Tables 1* and *2*).

Such results support the conclusion that in the PA6 matrix the lowest molecular mass of the EVA copolymers could be dissolved and that such a dissolution may be promoted by increasing the VAc content along the copolymer chain.

The X_c values of the PA6 phase crystallized in the presence of EVA copolymers are slightly lower than that of plain PA6 (see *Table 3*). It should be noted that, for blends containing the EVA copolymers having comparatively lower and higher molecular mass, the X_c values shown by PA6 phase depend on the EVA VAc content; the decrease becomes larger with increasing VAc content along the EVA copolymer chain. No systematic dependence of X_c(PA6) on EVA VAc content was found in the case of the blends containing EVA copolymer having intermediate molecular mass. On the other hand, for a given EVA VAc content X_c(PA6) values decrease with decreasing copolymer molecular mass (see *Tables 1* and *3*).

Structural analysis

It is well known that PA6 may crystallize from the melt in two different crystalline forms[9], namely α and γ, and that the nucleation, growth and relative amount of such forms depend on the crystallization conditions.

For the crystallization conditions imposed by the processing undergone by plain PA6 and PA6/EVA blends it was found that 32% of the plain PA6 crystallizes in γ form (see *Figure 1*). It is interesting to observe that I_γ values shown by PA6 crystallized in the presence of EVA copolymers are higher than that shown by plain PA6 (see *Figure 1*). Such results could suggest that the EVA copolymers may act as a nucleating agent for γ crystalline form of PA6.

Table 3 Crystallinity index of PA6 phase (X_c(PA6)) and of PA6/EVA blends (X_c(blend)) of plain PA6 and PA6 crystallized from its blends with EVA copolymers

Code	X_c(blend) (%)	X_c(PA6) (%)
PA6	–	45
PA6/EVA1	38	42
PA6/EVA2	40	44
PA6/EVA3	34	37
PA6/EVA4	36	40
PA6/EVA5	37	41
PA6/EVA6	40	44
PA6/EVA7	37	42

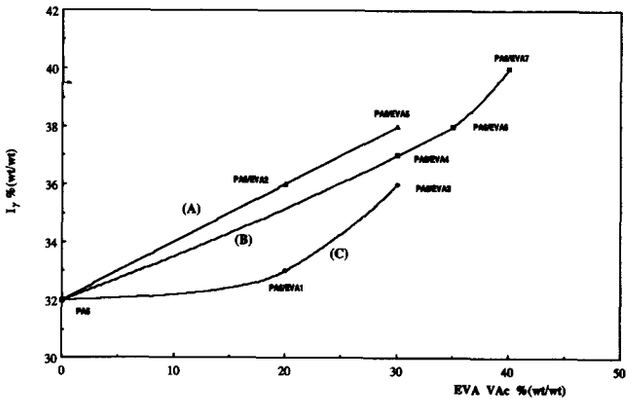

Figure 1 The γ form index *versus* EVA VAc content for plain PA6 and PA6/EVA blends. Curves: (A) EVA2 and EVA5 containing blends; (B) EVA4, EVA6 and EVA7 containing blends; (C) EVA1 and EVA3 containing blends

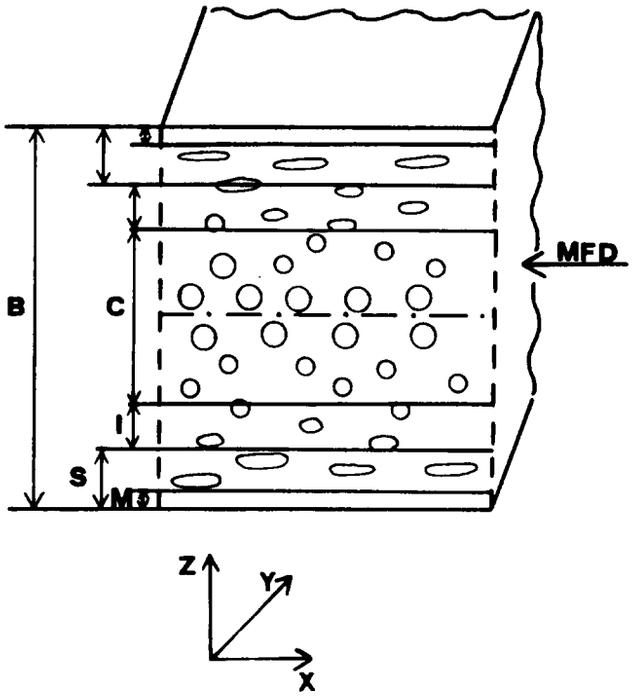

Figure 2 Schematic model of the layered structure shown by all examined samples of PA6/EVA blends in direction perpendicular to the melt flow direction. Symbols: B, thickness of the sheet (1 mm); C, core; I, intermediate layer; M, surface matrix layer; S, skin; MFD, mould flow direction

It should be noted, moreover, that, for a given EVA molecular mass, I_γ increases with increasing VAc content along the copolymer chain (see *Figure 1*) and that for a given EVA VAc content I_γ increases with increasing EVA molecular mass.

From the above, one could infer that the capability of the EVA copolymer to nucleate γ crystalline form increases with increasing both VAc content along its chain and molecular mass.

The highest I_γ value (40%) is shown by the blend containing the copolymer having the highest VAc content along its chain and intermediate molecular mass.

Mode and state of dispersion of the minor component

The analysis by SEM of the mode and state of EVA dispersion into the polyamide matrix, performed on smoothed and subsequently etched transversal and longitudinal surfaces of the dumbbell-shaped specimen of the PA6/EVA blends, reveals a layered structure according to the schematic model reported in *Figure 2*. One should recall that an anisotropic distribution of EVA dispersed phase into PA6 matrix has already been observed while studying extruded[1] and injection-moulded[2] samples. As a matter of fact the EVA particle size and the concentration of the EVA particles were found to increase with characteristic gradient on moving from the skin towards the core of the sample for both extruded and moulded samples.

As shown in *Figure 2*, and in agreement with the results reported in the previous work dealing with PA6/EVA injection-moulded samples[3], at the outer skin of the sample no domains of dispersed phase are observable. The presence of an outer skin layer presumably containing no copolymer could be explained by preferential wetting of the mould wall with the PA6 as proposed by Southern and Ballman[10]. The thickness of such a layer (M), which looks free of EVA domains, is reported in *Tables 4–6* for all the blends examined. As shown, such thickness measures about 1 μm for all examined samples; the only

Table 4 Layered distribution in injection-moulded samples of PA6/EVA blends with reference to *Figure 2*. Layer code, layer thickness, shape and size of the EVA domains for: (A) PA6/EVA1 and (B) PA6/EVA3 blends

Layer code	Layer thickness (%)	Shape of EVA domains	Size of EVA domains (μm)
M	(A) 1.3	–	–
	(B) 0.9	–	–
S–M	(A) 6	Fibre	Breadth = 0.6–1.0 Length = 2–14
	(B) 7	Ellipsoidal	Minor axis = 0.8–2 Major axis = 1.6–9.8
I	(A) 8	Ellipsoidal and spherical	Minor axis = 0.8–1.2 Major axis = 2.2–9.6 Spherical = 0.2–0.8
	(B) 12	Ellipsoidal	Minor axis = 0.6–1.2 Major axis = 1.2–4.2
C	(A) 35	Spherical	0.8–4
	(B) 31	Spherical	0.8–4

Table 5 Layered distribution in injection-moulded samples of PA6/EVA blends with reference to *Figure 2*. Layer code, layer thickness, shape and size of the EVA domains for: (C) PA6/EVA4, (D) PA6/EVA6 and (E) PA6/EVA7 blends

Layer code	Layer thickness (%)	Shape of EVA domains	Size of EVA domains (μm)
M	(C) 2.4	–	–
	(D) 1.0	–	–
	(E) 0.8	–	–
S–M	(C) 10	Ellipsoidal	Minor axis = 0.2–0.4 Major axis = 0.6–1.6
	(D) 7	Spherical	0.2–0.6
	(E) 10	Ellipsoidal	Minor axis = 0.6–1.2 Major axis = 1.4–6
I	(C) 9	Spherical	0.4–1.0
	(D) 5	Spherical	0.2–1.0
	(E) 5	Ellipsoidal and spherical	Minor axis = 0.6–1.0 Major axis = 2.4–4.4 Spherical = 0.2–0.8
C	(C) 29	Spherical	0.6–2.6
	(D) 37	Spherical	0.8–2.0
	(E) 34	Spherical	0.8–2.4

Table 6 Layered distribution in injection-moulded samples of PA6/EVA blends with reference to *Figure 2*. Layer code, layer thickness, shape and size of the EVA domains for: (F) PA6/EVA2 and (G) PA6/EVA5 blends

Layer code	Layer thickness (%)	Shape of EVA domains	Size of EVA domains (μm)
M	(F) 0.8	–	–
	(G) 0.9	–	–
S–M	(F) 6	Ellipsoidal	Minor axis = 0.4–1.2 Major axis = 1.6–9.2
	(G) 2	Ellipsoidal	Minor axis = 0.2–0.6 Major axis = 0.8–2.8
I	(F) 15	Ellipsoidal	Minor axis = 0.6–1.2 Major axis = 1.6–5.0
	(G) 5	Spherical	0.4–1.6
C	(F) 28	Spherical	0.6–4.0
	(G) 42	Spherical	0.8–4.0

EVA4 containing blend, in fact, exhibits a comparatively thicker M layer (2.4 μm).

Moving toward the core of the sample a layer ($S-M$) is found (see *Figure 2*), where the dispersed EVA particles are more or less elongated along the flow direction assuming an ellipsoidal and/or cylindrical shape. Note that the observed deformation of the dispersed phase particles verifies the flow pattern proposed by Tadmor[11] on the observation of Rose[12]. According to the Tadmor model containing both elongational and shear flow fields, the fountain or volcano effect of the advancing flow front deforms the particles of the minor component along the flow direction.

From the analysis of the thickness of the layer ($S-M$) and of the extent of deformation undergone in such a layer by the domains of EVA copolymers having almost the same melt viscosity, the following comments can be made:

(i) In the case of blends containing the copolymers having comparatively lower melt viscosity (EVA1 and EVA3), slightly higher thickness is shown by the EVA3 containing blend (see *Table 4*). It should be pointed out that the EVA1 copolymer forms rods parallel to the flow direction whereas EVA3 copolymer segregates in ellipsoidal shaped domains (see *Figure 3*). The lengths of EVA1 rubbery rods are in the range 2–14 μm and their thickness is about 0.8 μm. On the other hand, the minor and major axes of EVA3 ellipsoids are in the ranges 0.8–2 μm and 1.6–9.8 μm respectively. Such morphological results indicate that EVA3 copolymer offers higher resistance to deformation than that shown by EVA1 copolymer. Taking into account that EVA1 and EVA3 copolymers have almost the same melt viscosity, their different states of dispersion could be related to the VAc content along the copolymer chain. It could be that an increase of VAc content from 20% wt/wt (EVA1) to 30% wt/wt (EVA3) results in an increased elasticity of the EVA copolymer.

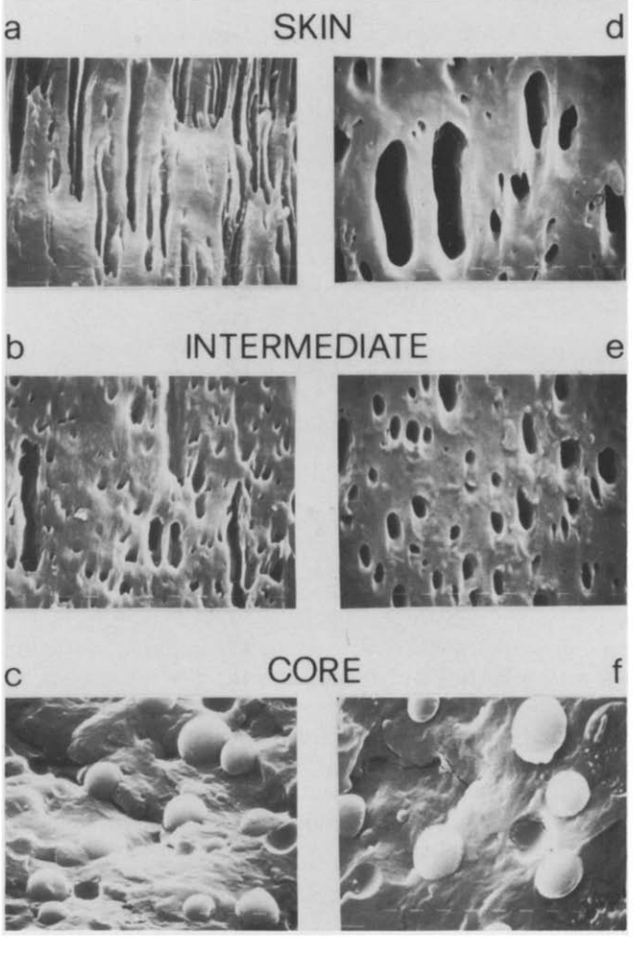

Figure 3 Influence of VAc content (EVA MFI = 300–500 (g 10 min^{-1})). Scanning electron micrographs of smoothed surfaces exposed to boiling xylene vapour and of cryogenic fracture surfaces for PA6/EVA1 90/10 (a,b,c) and PA6/EVA3 90/10 (d,e,f) blends: (i) etched surface (a,b,d,e) (1800 ×); (ii) cryogenic fracture surface (c,f) (1800 ×)

(ii) Among the blends containing copolymers having intermediate melt viscosity (EVA4, EVA6 and EVA7) (see *Table 5*), EVA4 and EVA7 containing blends exhibit quite comparable $S-M$ values, whereas for the blend containing EVA6 copolymer the $S-M$ results are lower. It should be underlined that in such a layer EVA6 segregates in almost spherical shaped domains with a diameter lower than 1 μm whereas EVA4 and EVA7 form ellipsoidal shaped domains (see *Figure 4*). It is to be noted, moreover, that the ranges of the minor and major axes of EVA4 ellipsoids are respectively narrower (0.2–0.4 μm and 0.6–1.6 μm) than that shown by EVA7 ellipsoids (0.6–1.2 μm and 1.4–6 μm). From the above it comes out that an increase of the VAc content from 30% wt/wt (EVA4) to 35% wt/wt (EVA6) along the copolymer chain induces a higher resistance to deformation and a finer dispersion of the EVA minor component. Contrary to expectation, by further increasing the VAc content up to 40% wt/wt (PA6/EVA7), the resistance to deformation and the dispersion coarseness shown by EVA7 phase respectively become lower and higher than that shown by the copolymer having 30% wt/wt of VAc (PA6/EVA4).

(iii) For the blends containing copolymer having comparatively higher melt viscosity (EVA2 and EVA5), the EVA2 containing blends show a $S-M$ layer whose thickness is about three times as large as that shown by EVA5 containing blend (see *Table 6*). Moreover, as shown in *Figure 5* and by comparison between the ranges of the minor and major axes of the ellipsoidal shaped domains respectively formed by both copolymers (0.4–1.2 μm, 1.6–9.2 μm and 0.2–0.6 μm, 0.8–2.8 μm), the EVA5 dispersed phase exhibits a resistance to deformation higher than that shown by the EVA2 copolymer. In agreement with results already observed for blends containing EVA copolymer of lower melt viscosity, it seems that an increase of VAc content along the EVA chain from 20% up to 30% wt/wt results in increased copolymer elasticity.

Looking at the influence of the EVA melt viscosity on the mode and state of dispersion and on the deformation undergone by the domains of the minor component in $S-M$ layer, the following observations can be made:

(i) For a VAc content of 20% wt/wt, on increasing EVA molecular mass a drastic change in the state of dispersion of the copolymer is observed. As shown in *Figure 6*, rods are formed by EVA with lower molecular mass whereas EVA with higher molecular mass segregates into ellipsoidal shaped domains. Such findings indicate, moreover, that the EVA copolymer of higher molecular mass shows a higher resistance to deformation.

(ii) For an EVA with a VAc content of 30% wt/wt (see *Figure 7*) the coarsest and finest dispersion are shown by the blends containing the EVA copolymer of lower and intermediate molecular mass respectively (compare *Figures 7a, 7d* and *7g*). The dispersion coarseness of the

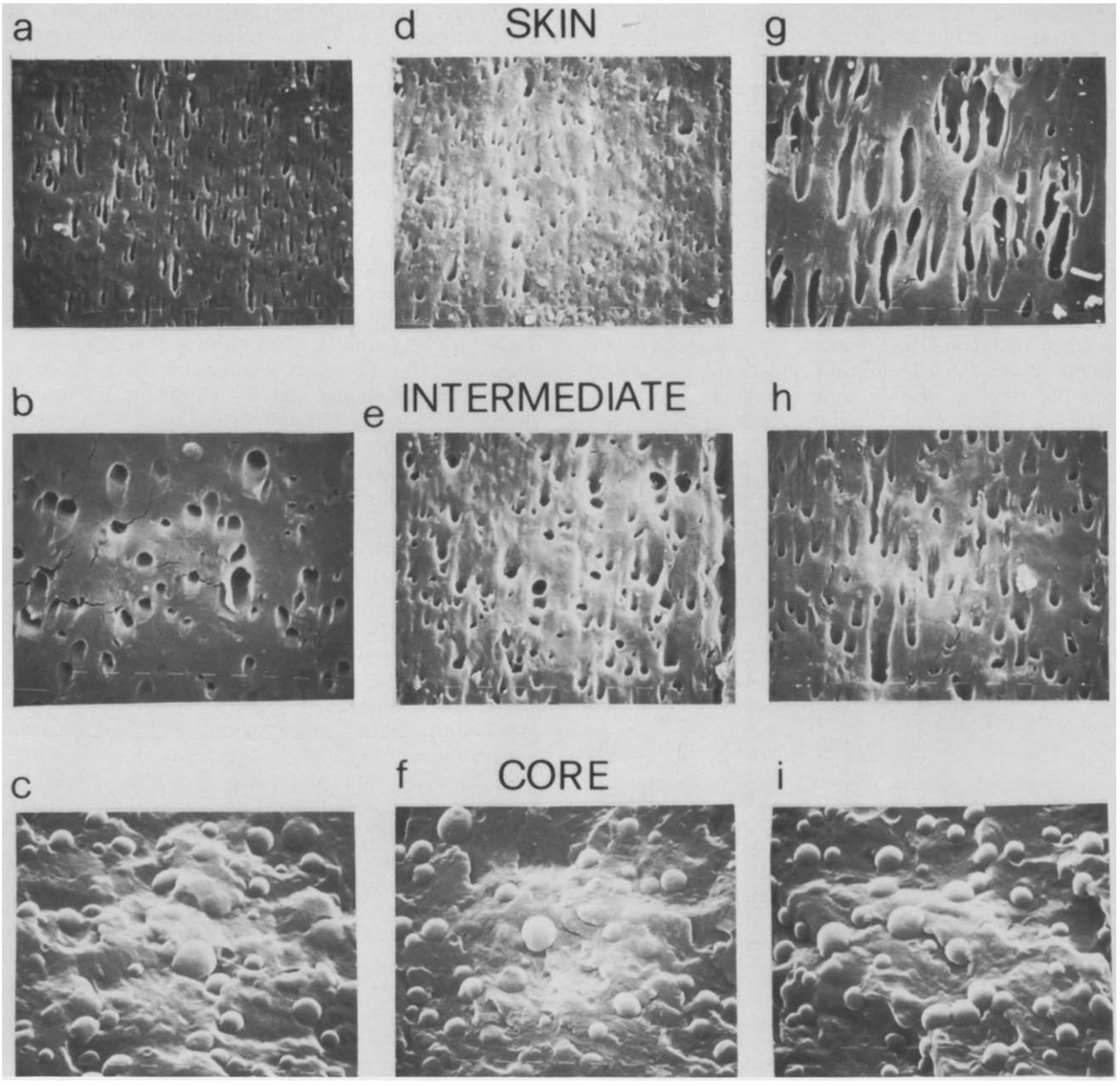

Figure 4 Influence of VAc content (EVA MFI = 30–40 (g 10 min^{-1})). Scanning electron micrographs of smoothed surfaces exposed to boiling xylene vapour and of cryogenic fracture surfaces for PA6/EVA4 90/10 (a,b,c), PA6/EVA6 90/10 (d,e,f) and PA6/EVA7 90/10 (g,h,i) blends: (i) etched surface (a,b,d,e,g,h) (2500 ×); (ii) cryogenic fracture surface (c,f,i) (2500 ×)

EVA copolymer of higher molecular mass is higher than that developed in the blend containing the copolymer of intermediate molecular mass. Moreover, as occurs in the case of PA6/EVA blends containing the copolymer having 20% wt/wt of VAc along the chain, higher deformation is undergone by the domains of EVA copolymer of lower molecular mass (compare *Figures 6* and *7*). From the above it may be deduced that higher deformations are to be associated with both lower melt viscosity and lower VAc content along the EVA chain (20% wt/wt).

Moving further on towards the core of the PA6/EVA samples, the rod-like and/or ellipsoidal EVA shaped domains tend to assume a more or less spherical shape (see layer *I* in *Figure 2*). The thickness of such a layer *I*, shown by blends containing EVA copolymer having comparatively lower melt viscosity (EVA1 and EVA3), was found to increase with increasing VAc content along the copolymer chain (see *Table 4*). On the contrary for blends containing EVA copolymer of comparatively higher melt viscosity the thickness of the *I* layer decreases on increasing the EVA VAc content (compare the *I* value shown by PA6/EVA2 blend with the *I* value shown by PA6/EVA5 blend and also the *I* value shown by PA6/EVA4 blend with the *I* value shown by PA6/EVA7 blend) (see *Tables 5* and *6*).

As for the extent of deformation undergone in such a layer (see *Figure 2*) by domains of EVA copolymer having almost the same melt viscosity, the following observations can be made:

(i) For the blend containing comparatively minor EVA component of lower melt viscosity (EVA1 and EVA3), the EVA1 rods disappear (compare *Figures 3a* and *3b*) and almost spherical and ellipsoidal shaped domains are formed. The average diameter of EVA1 particles is about 0.2–0.8 μm and the minor and major axes of the ellipsoids

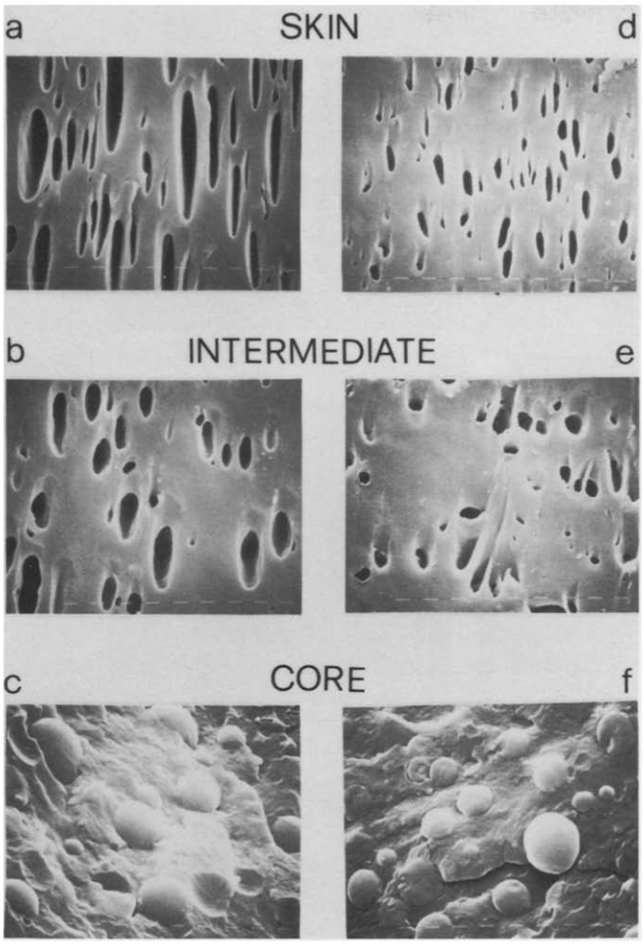

Figure 5 Influence of VAc content (EVA MFI = 3–4 ($g\,10\,min^{-1}$)). Scanning electron micrographs of smoothed surfaces exposed to boiling xylene vapour and of cryogenic fracture surfaces for PA6/EVA2 90/10 (a,b,c) and PA6/EVA5 90/10 (d,e,f) blends: (i) etched surface (a,b,d,e) (1800 ×); (ii) cryogenic fracture surface (c,f) (1800 ×)

are in the following ranges: 0.8–1.2 μm and 2.2–9.6 μm. In the case of EVA3 containing blend the range of the minor axis is quite comparable to that shown by EVA1 copolymer, whereas the range of the major axis is narrower (1.2–4.2 μm) than that shown by EVA1 copolymer (see *Figure 3*).

(ii) For the blends containing the copolymers of intermediate molecular mass (EVA4, EVA6 and EVA7), the EVA4 and EVA6 phase is dispersed in spherical shaped domains with diameters ranging between 0.4 and 1.0 μm and 0.2 and 1.0 μm, respectively. In the case of the blend containing EVA7 copolymer, both ellipsoidal and spherical shaped domains are observed. The minor and major axes of the ellipsoids and the diameter of the particle are respectively contained in the following ranges: 0.6–1.0 μm, 2.4–4.4 μm and 0.2–0.8 μm. It is to be noted that the size of the spherical shaped domains of the minor component tend to decrease slightly with increasing VAc content along the EVA chain.

(iii) For the blends containing the copolymers of comparatively higher molecular mass (EVA2 and EVA5) the ellipsoidal shaped domains formed by EVA copolymer have average minor and major axes contained in the ranges 0.6–1.2 μm and 1.6–5.0 μm, whereas EVA5 copolymer segregates into almost spherical shaped domains with a diameter ranging between 0.4 and 1.6 μm.

Looking at the influence of EVA melt viscosity on the mode and state of dispersion of the minor component, it can be seen that for a vinyl acetate content of 20% wt/wt along the copolymer chain (EVA1 and EVA2) on increasing the EVA molecular mass the range of the major axis of the ellipsoidal shaped domains decreases (compare *Figures 7a* and *7b*). As a matter of fact the major axes of the domains of the copolymer having lower (EVA1) and higher (EVA2) molecular mass are respectively contained in the following ranges: 2.2–9.6 and 1.6–5.0 μm. Such results indicate that the dispersion coarseness and the deformation undergone in the *I* layer by such minor components increase with increasing EVA molecular mass.

Also in the case of PA6/EVA blends containing copolymers having 30% wt/wt of VAc along their chain (PA6/EVA3, PA6/EVA4 and PA6/EVA5), the state of dispersion of the minor component depends strongly on EVA molecular mass. As shown in *Figures 7b, 7e* and *7h* the copolymer of lower molecular mass (PA6/EVA3) segregates in the *I* layer into ellipsoidal shaped domains (minor and major axes 0.6–1.2 μm and 1.2–4.2 μm), whereas spherical shaped domains are formed by the copolymer with higher molecular mass (PA6/EVA4 and PA6/EVA5). The finest dispersion of the minor component is developed in the blend containing the copolymer of intermediate molecular mass (EVA4), whose particle size ranges between 0.4 and 1.0 μm; for the copolymer

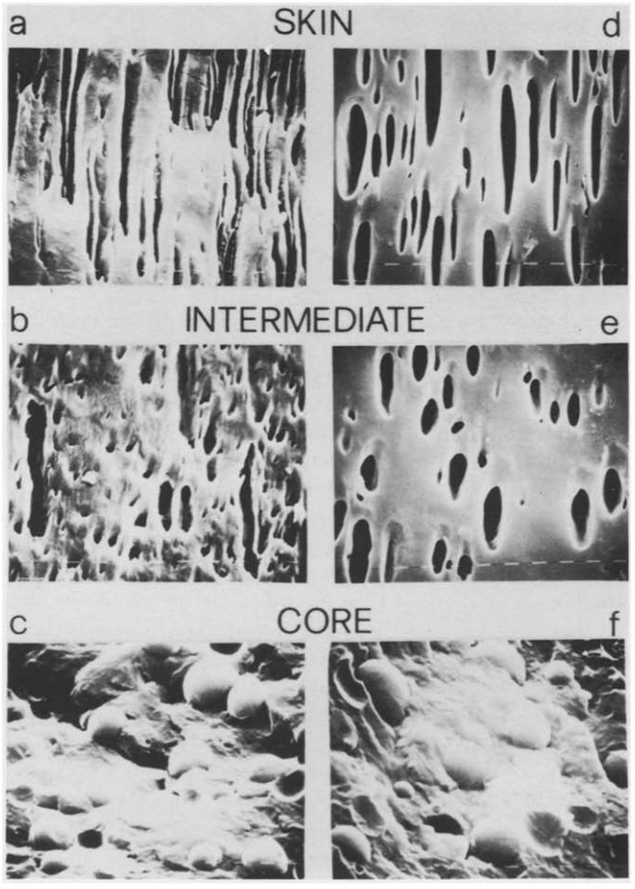

Figure 6 Influence of EVA MFI (VAc content = 20%). Scanning electron micrographs of smoothed surfaces exposed to boiling xylene vapour and of cryogenic fracture surfaces for PA6/EVA1 90/10 (a,b,c) and PA6/EVA2 90/10 (d,e,f) blends: (i) etched surface (a,b,d,e) (2000 ×); (ii) cryogenic fracture surface (c,f) (2000 ×)

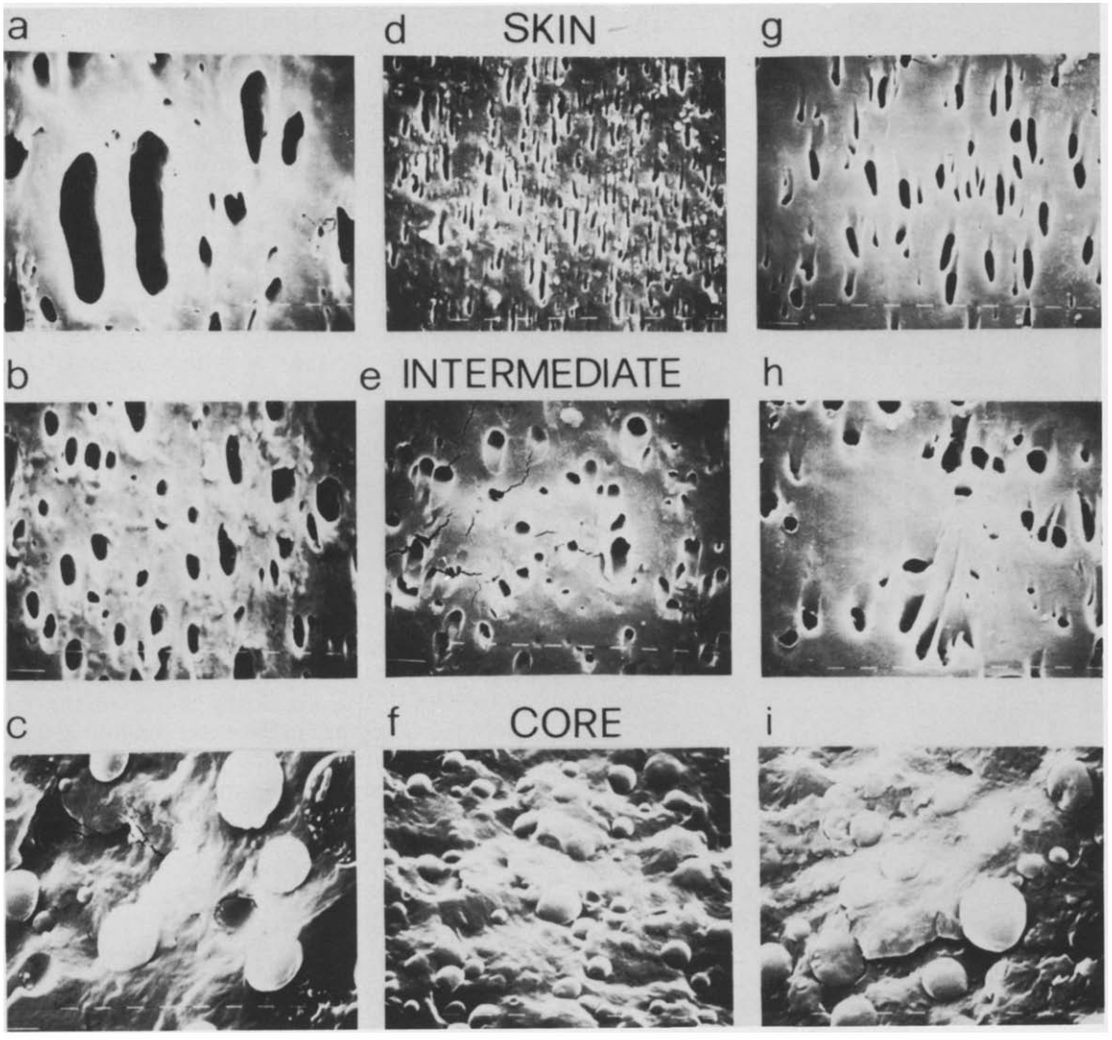

Figure 7 Influence of EVA MFI (VAc content = 30%). Scanning electron micrographs of smoothed surfaces exposed to boiling xylene vapour and of cryogenic fracture surfaces for PA6/EVA3 90/10 (a,b,c), PA6/EVA4 90/10 (d,e,f) and PA6/EVA5 90/10 (g,h,i) blends: (i) etched surface (a,b,d,e,g,h) (2300 ×); (ii) cryogenic fracture surface (c,f,i) (2300 ×)

with highest molecular mass (EVA5) the range is in fact slightly wider (0.6–1.6 μm).

Such results indicate, in agreement with results already observed in the case of PA6/EVA blends containing the copolymer having 20% wt/wt of VAc along the chain, that for a given VAc content along the copolymer chain the dispersion coarseness and the deformation undergone by the domains of the minor component tend to decrease with increasing EVA molecular mass.

Moving on to the core of the dumbbell-shaped specimens a droplet-like morphology is observed (see *Figure 2*). In the case of blends containing EVA copolymer having comparatively lower and higher melt viscosity (EVA1, EVA3 and EVA2, EVA5) the particle size ranges between 0.8 and 4.0 μm. A finer dispersion of the EVA minor component is developed in the blend containing the copolymer of intermediate melt viscosity (EVA4, EVA6 and EVA7) (compare *Figures 4c, 4f, 4i* with *Figures 3c, 3f* and *5c, 5f*). As a matter of fact in such blends the largest particles have an average diameter of 2.5 μm.

Such results indicate that in the core of the samples, at least, irrespective of VAc content along the copolymer chain, a finer dispersion is developed in the blend containing EVA copolymer of intermediate melt viscosity. Such a result agrees with that already obtained while studying injection-moulded samples of different PA6/EVA blends[2].

Elastic modulus and yielding behaviour

Stress–strain curves for plain PA6 and PA6 crystallized in the presence of EVA copolymers up to the yield point are shown in *Figure 8*. The values of the elastic modulus E, the stress at yield σ_y and the elongation at yield ε_y for the plain PA6 and PA6/EVA blends are reported in *Table 7* together with the EVA melt index and VAc content. It can be observed that the elastic behaviour of PA6/EVA blends is strongly dependent on the EVA molecular characteristics. As a matter of fact, for lower VAc content along the copolymer chain (20% wt/wt) PA6/EVA1 and PA6/EVA2 containing blends exhibit the same E value, irrespective of EVA molecular mass. As expected, taking into account the copolymer contribution, such values are lower than that shown by plain PA6. It would be surprising to observe that an increase of the VAc content along the copolymer chain from 20% up to 30% wt/wt (EVA3, EVA4 and EVA5) results in an increased modulus (see *Figure 8* and *Table 7*). It should be noted, furthermore, that the extent of such an increase depends on the EVA molecular mass. For blends

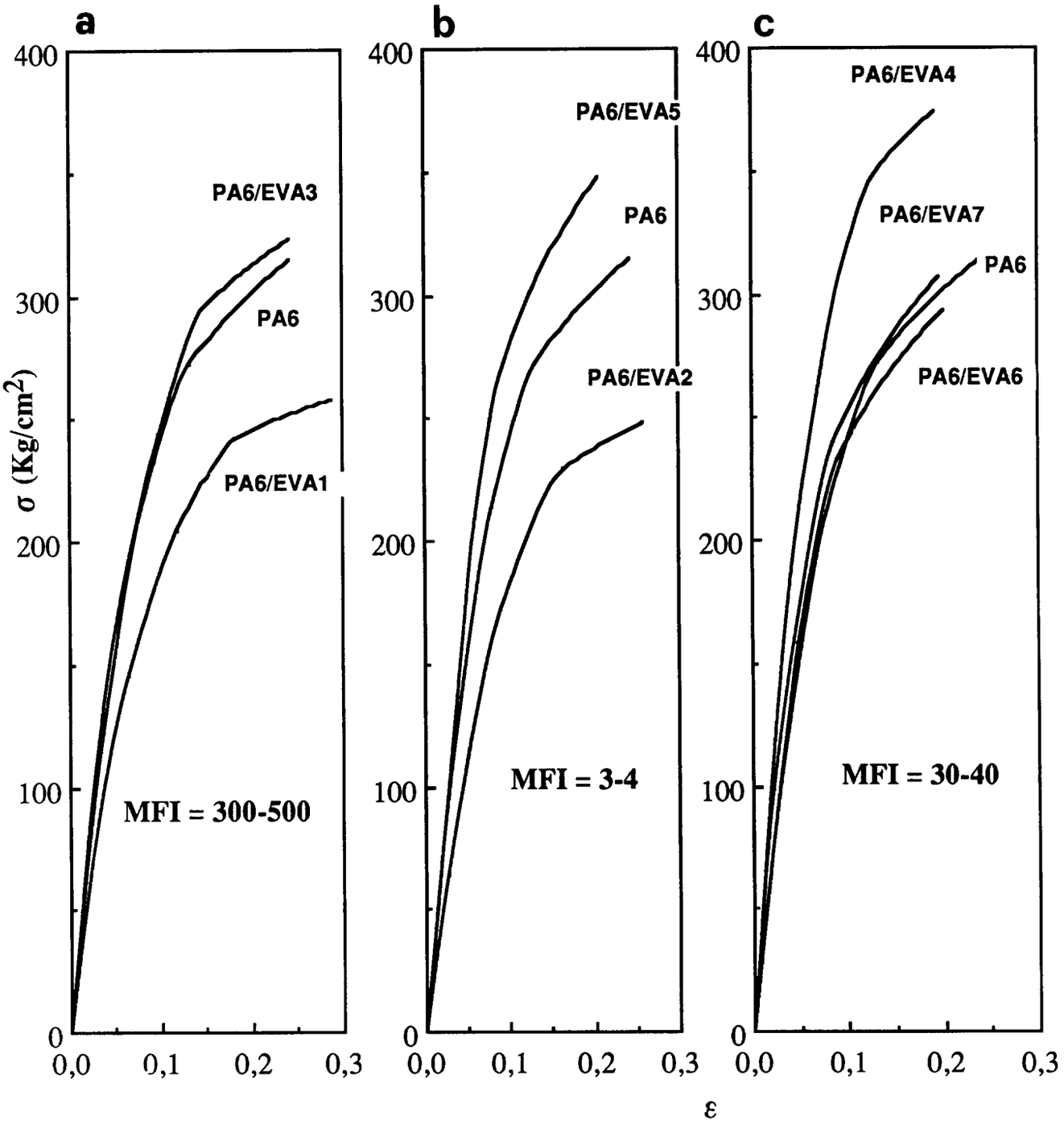

Figure 8 Stress–strain curves for the plain PA6 and PA6/EVA blends up to yield point: (a) pure PA6 and EVA1, EVA3 containing blends; (b) pure PA6 and EVA2, EVA5 containing blends; (c) pure PA6 and EVA4, EVA6, EVA7 containing blends

Table 7 Moduli (E), stress at yield (σ_y), elongation at yield (ε_y) and molecular characteristics of pure PA6 and PA6/EVA blends

Code	$E \times 10^3$ (kg cm^{-2})	$\sigma_y \times 10^2$ (kg cm^{-2})	ε_y	EVA melt index (g/10 min)	Vinyl acetate (%wt/wt)
PA6	3.5±0.2	3.1±0.03	0.24±0.004	–	–
PA6/EVA1	2.5±0.3	2.5±0.2	0.27±0.01	300–500	20
PA6/EVA2	2.7±0.2	2.5±0.2	0.23±0.01	3–4	20
PA6/EVA3	3.6±0.2	3.1±0.1	0.24±0.006	300–500	30
PA6/EVA4	4.4±0.6	3.6±0.3	0.22±0.01	30–40	30
PA6/EVA5	4.2±0.4	3.4±0.2	0.20±0.005	3–4	30
PA6/EVA6	3.6±0.2	3.0±0.1	0.19±0.005	30–40	35
PA6/EVA7	3.7±0.3	3.1±0.2	0.19±0.003	30–40	40

containing copolymers of lower molecular mass (EVA1 and EVA3) the modulus of the blended material rises up to the value shown by plain PA6, whereas a modulus higher than that shown by plain PA6 is exhibited by the blends containing the copolymer having higher molecular mass (EVA4 and EVA5).

By further increase of VAc content along the EVA chain (35% and 40% wt/wt), no further increase is observed. PA6/EVA6 and PA6/EVA7 blends, in fact, show E values quite comparable to that shown by PA6/EVA3 blend, that is the modulus of plain PA6.

Such results seem to indicate that the 30% wt/wt of VAc content along the EVA chain could be an optimal content in order to obtain a blended material with an elastic modulus quite comparable with or even higher than that shown by plain PA6.

As shown by comparing *Figure 9* with *Figure 10*, which report respectively the trend of the E values *versus* VAc content of EVA copolymer and the trend of the ratio E/X_c(blend) *versus* VAc content for all investigated blends, the trend of the ratio E/X_c(blend) is quite analogous to that of E, indicating that the modulus and the crystallinity are not directly proportional.

As expected the trend shown by the strength at yield

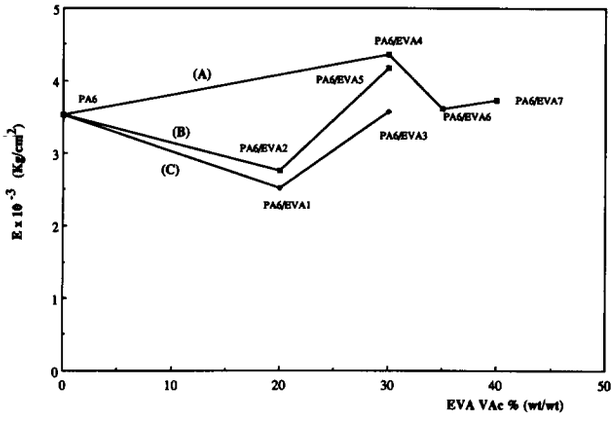

Figure 9 Modulus *versus* VAc content of EVA copolymer for the plain PA6 and PA6/EVA blends. Curves: (A) EVA4, EVA6 and EVA7 containing blends; (B) EVA2 and EVA5 containing blends; (C) EVA1 and EVA3 containing blends

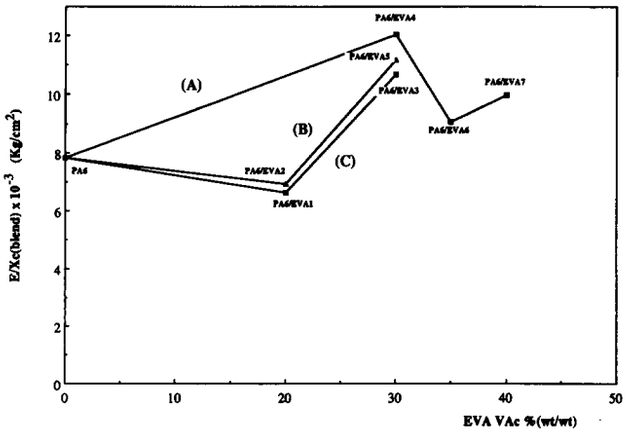

Figure 10 Ratio between the modulus E and the crystallinity index values of plain PA6 (X_c(PA6)) and PA6/EVA blends (X_c(blend)) *versus* VAc content of EVA copolymer for the plain PA6 and PA6/EVA blends. Curves: (A) EVA4, EVA6 and EVA7 containing blends; (B) EVA2 and EVA5 containing blends; (C) EVA1 and EVA3 containing blends

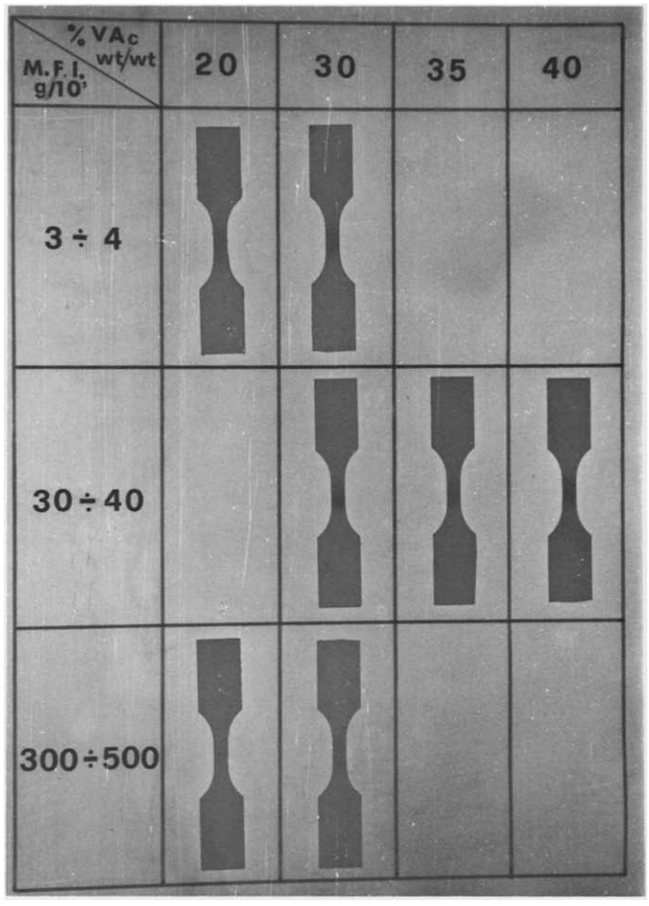

Figure 11 Photograph of dumbbell-shaped specimens of plain PA6 and PA6/EVA blends at the yield point, together with the *MFI* and VAc content of the EVA copolymers

σ_y of PA6/EVA blends is analogous to that shown by the elastic modulus (see *Table 7*). The blends containing EVA copolymer having 20% wt/wt of VAc along their chain (PA6/EVA1 and PA6/EVA2), irrespective of molecular mass, exhibit the same σ_y value and this value is lower than that shown by plain PA6. The PA6/EVA3, PA6/EVA6 and PA6/EVA7 blends show the same σ_y values as shown by plain PA6, whereas PA6/EVA4 and PA6/EVA5 exhibit a σ_y value higher than that shown by plain PA6.

As far as ε_y values are concerned, it can be observed that PA6/EVA3 and PA6/EVA1 blends show respectively ε_y values quite comparable to and higher than that shown by plain PA6, whereas all the remaining PA6/EVA blends show ε_y values lower than that shown by plain PA6.

It is interesting to observe that the ε_y values, for a given EVA molecular mass, tend to decrease with increasing VAc content along the EVA chain (see *Table 7*) and that, for a given VAc content, ε_y increases with decreasing EVA molecular mass (see *Table 7*).

It was, moreover, found that no stress whitening at the σ_y value is shown by dumbbell-shaped specimens of plain PA6 and PA6/EVA1 blend. On the other hand, all the remaining samples of PA6/EVA blends show in the central part a more or less stress-whitened zone depending on the EVA molecular structure (see *Figure 11*). As shown, for lower VAc content along the copolymer chain (20% wt/wt) a slight stress-whitening phenomenon takes place only in samples of the blend containing the EVA

copolymer with higher molecular mass (PA6/EVA2 blend). With increasing VAc content to 30% wt/wt the stress-whitening phenomenon tends to increase with an intensity strongly dependent on EVA molecular mass. As shown in *Figure 11* the greatest and the least stress-whitening phenomena are shown by the blends containing the EVA copolymer of intermediate and lower molecular mass respectively (PA6/EVA4 and PA6/EVA3). A stress-whitening phenomenon more or less pronounced than that respectively shown by PA6/EVA3 and PA6/EVA4 blends is undergone by the blend containing the EVA copolymer with higher molecular mass (PA6/EVA5). By further increasing the VAc content along the EVA chain, a slight decrease in stress-whitening phenomenon is observed for the samples of the blends containing the copolymer with intermediate molecular mass (compare PA6/EVA6 and PA6/EVA7 with PA6/EVA4).

The stress-whitening phenomenon is to be associated with multicraze formation and/or cavitation during the tensile tests. It is interesting to note that more pronounced stress whitening is shown by the blends in which a finer dispersion of the EVA minor component is developed (particle size ranging between 0.8 and 2.5 μm), PA6/EVA4, PA6/EVA6 and PA6/EVA7 blends, indicating that in the PA6 matrix smaller particles promote multicraze formation and/or a cavitation process. It is to be pointed out, furthermore, that for a given VAc content along the EVA chain, more intense stress whitening is undergone by the blends in which the minor component offers a higher resistance to deformation (see *Figure 8*), suggesting that mainly spherical shaped domains are able to initiate multicraze formation and/or are mechanically equivalent to a void taking into account the very weak adhesion at the interface[2].

CONCLUDING REMARKS

A study of the influence of molecular structure and composition of EVA copolymers on mode and state of dispersion developed in PA6 based blends during the injection-moulding process and on the elastic and tensile yielding behaviour of such materials has been reported.

All investigated samples show a layered structure in the direction perpendicular to mould flow direction. Moving from the border towards the core of the samples, the following four layers were found:

(1) An outer skin where no domains of EVA dispersed phase are observed. The presence of such a layer was already observed in a previous work[2] dealing with injection-moulded samples of PA6/EVA blends and could be due to the preferential wetting of the mould wall by the matrix.

(2) A skin where the EVA dispersed phase segregates into ellipsoidal and/or cylindrical shaped domains tangentially to the mould flow direction according to the flow pattern proposed by Tadmor[11]. In such a layer the mode and state of dispersion of the minor component are determined by both EVA molecular mass and VAc content along the copolymer chain. For the blends containing EVA copolymer having comparatively lower and higher molecular mass, the resistance to deformation was found to increase with increasing VAc content along the EVA chain from 20 to 30% wt/wt. For the blends containing EVA copolymers of intermediate molecular mass the resistance to deformation increased with increasing VAc content from 30 to 35% wt/wt. By further increasing the VAc content up to 40% wt/wt the deformation undergone by the EVA phase was considerably higher than that exhibited by the two remaining EVA copolymers having the same molecular mass. For a VAc content of 20% wt/wt along the EVA chain the copolymer having comparatively lower molecular mass forms rods parallel to the melt flow direction, whereas the EVA with higher molecular mass segregates into ellipsoidal shaped domains. For an EVA VAc content of 30% wt/wt coarser and finer dispersions of the minor component are shown by the blends containing the EVA copolymer of lower and intermediate molecular mass respectively. Higher deformation of the EVA domains along the melt flow direction are associated with both lower melt viscosity and lower VAc content along the EVA chain (20% wt/wt).

(3) An intermediate layer where the ellipsoidal and/or cylindrical shaped domains tend to assume a more or less spherical shape.

(4) A core showing EVA droplet-like morphology to be ascribed presumably to the relaxation and/or breaking up of the previously formed EVA cylindrical and ellipsoidal shaped domains. In such a core the EVA particle size is determined by copolymer molecular mass, irrespective of VAc content. Finer dispersion of the minor component was found to develop in blends containing EVA of intermediate molecular mass according to results already obtained by us while studying injection-moulded samples of different PA6/EVA blends. Moreover, it came out that blends containing EVA copolymers with comparatively lower and higher melt viscosity show the same range of particle size.

The elastic behaviour of PA6/EVA blends was strongly dependent on the EVA molecular characteristics. For lower VAc content along the copolymer chain (20% wt/wt), irrespective of EVA molecular mass, the blended material shows the same modulus lower than that exhibited by plain PA6. By increasing the VAc content along the EVA chain up to 30% wt/wt, the elastic modulus increases. For blends containing copolymers of lower molecular mass, the modulus rises up to the value shown by plain PA6, whereas a modulus higher than that shown by plain PA6 is exhibited by the blends containing the copolymer having higher molecular mass. On further increase of VAc content along the EVA chain, no further E increase was observed.

At yield, no stress whitening is shown by a dumbbell-shaped specimen of plain PA6 and of the blends containing EVA copolymer with both lower molecular mass and VAc along its chain. All the remaining samples of PA6/EVA blends show, on the contrary, in the central part a more or less intense, stress-whitened zone, suggesting multicraze formation and/or a cavitation process. It was, moreover, observed that more pronounced stress whitening is undergone by the blends in which a finer dispersion of the EVA minor component is developed.

ACKNOWLEDGEMENT

This work was partly supported by Progetto Finalizzato Chimica Fine II of Italian CNR.

REFERENCES

1 D'Orazio, L., Mancarella, C., Martuscelli, E., Casale, A., Filippi, A. and Speroni, F. *J. Mater. Sci.* 1986, **21**, 989

2 D'Orazio, L., Mancarella, C., Martuscelli, E., Casale, A., Filippi, A. and Speroni, F. *J. Mater. Sci.* 1987, **22**, 429
3 Addonizio, M. L., D'Orazio, L., Mancarella, C., Martuscelli, E., Casale, A. and Filippi, A. *J. Mater. Sci.* 1989, **24**, 2939
4 Fujimura, T. and Iwakura, K. *Int. Chem. Eng.* 1970, **10**, 683
5 Utraki, L. A. and Kamal, M. R. *Polym. Eng. Sci.* 1982, **22**, 96
6 Cimmino, S., D'Orazio, L., Greco, R., Maglio, G., Malinconico, M., Mancarella, C., Martuscelli, E., Palumbo, R. and Ragosta, G. *Polym. Eng. Sci.* 1984, **24**, 48
7 Dole, M. and Wunderlich, B. *Makromol. Chem.* 1959, **34**, 29
8 Kyotani, M. and Mitsuhashi, S. *J. Polym. Sci.* (*A-2*) 1972, **10**, 1497
9 Holmes, R., Bunn, C. W. and Smith, D. J. *J. Polym. Sci.* 1955, **17**, 159
10 Southern, J. H. and Ballman, R. L. *J. Appl. Polym. Sci.* 1979, **24**, 693
11 Tadmor, Z. *J. Appl. Polym. Sci.* 1974, **18**, 1753
12 Rose, W. *Nature* 1961, **191**, 242